Chapter 4

Geminal bis-ureas: gelation properties and structural studies in solution, in the gel state and in the solid state[1]

4.1 Introduction

Low molecular weight organic gelling agents are currently the subject of much attention, both because of the numerous applications of gels, and also because gelation phenomena by low molecular weight organic gelling agents are still poorly understood.[2,3,4] The molecular structures of known (very potent) organogelators are, however, very diverse, and often structurally closely related compounds do not exhibit any gelation properties. Most of the research has thus been focussed on exploring the molecular diversity of organogelators.

A different approach towards a better understanding of organogels and the elucidation of the molecular prerequisites for gelation to occur is through systematic design of novel organogelators. Recently, Hanabusa and our group independently demonstrated that bis-urea-based compounds are exceptionally well-suited for the design of low-molecular weight gelators owing to the rigidity, strength and high directionality of the multiple intermolecular hydrogen bonds that can be formed.[5,6] A key feature in the design of novel gelators are unidirectional gelator-gelator interactions, as is most clearly the case in *trans*-1,2-bisureidocyclohexane and 1,2-bisureidobenzene gelators (see also Chapter 3).[7] Due to the proximity of the urea groups in these molecules a coplanar orientation is preferred, which strongly favours one-dimensional aggregation through hydrogen bond formation. However, molecular modeling studies and experimental results indicate that one-dimensional aggregation by these compounds is prone to polymorphism, although the 1,2-bisureidocyclohexane and 1,2-bisureido-benzene gelating scaffolds have little conformational freedom and up to now the actual or dominant aggregate structures within gels are not known. So the question is: is it possible to establish a clear relationship between crystal structure, gel structure, aggregation in solution and monomer structure? Reports on crystal structures of gelator molecules have been scarce up to now[7b,8,9] and in one of those cases it could be demonstrated that the arrangement of gelator molecules in the crystal does not correspond fully with the molecular arrangement in a gel (see also Chapter 3).[7b]

In the present work we turned our attention to novel geminal bis-urea compounds. For geminal bis-ureas it is expected that there is not much independent rotational freedom of the two urea fragments due to their proximity, as is the case for 1,2-bisureidocyclohexane and 1,2-bisureidobenzene derivatives. It is very likely that the hydrogen bonding ability is directed along one intermolecular axis and should therefore strongly favour one-dimensional aggregation. The possible gelation of organic solvents by geminal bis-urea compounds will thus support the idea that unidirectional interactions are a prerequisite for gelation. This knowledge will be of great value to elucidate the structural requirements for gelation by other types of gelling agents for which in a first approximation the directionality of intermolecular interactions is less well defined as with the hydrogen bonding systems like these bis-urea compounds.

The second aim of this research on geminal bis-ureas is to obtain insight in the relationship between conformation and aggregation. Here we report on the synthesis of geminal bis-urea compounds and their gelation capability for organic solvents, as well as molecular modeling and solution and solid state NMR studies on their aggregation behaviour in solution and on the structure of the gels.

4.2 Synthesis

The synthesis of compounds **4.1 - 4.6** was based on a literature procedure for the preparation of geminal bis-acetamides.[10] This entails an in principle rather straightforward acid-catalysed condensation of a benzaldehyde and a monoalkylurea in refluxing toluene with azeotropic removal of water (Scheme 4.1). It was observed that usually a gel is formed during the reaction, which prevents 100% conversion to the desired product. In most cases, the use of lower reactant concentrations solves this problem. Upon cooling of the reaction mixture a precipitate or gel-like solid is formed, which could easily be isolated from the reaction mixture by filtration with suction. Suspending the product in a 50:50 mixture of dry dichloromethane and ether (together with some triethylamine) followed by ultrasound treatment and filtration yielded the desired products in pure form.

Attempts to synthesize bis-ureas with longer alkyl chains (octyl, dodecyl) were not successful. Although inspection of samples from these reaction mixtures by ^{1}H-NMR revealed that most of the starting materials had disappeared and product had formed, no product precipitated from the reaction mixture upon cooling to room temperature,

and all attempts to isolate it by other means failed. It those cases where products could be obtained by precipitation, it was found that these geminal bis-ureas are very sensitive to the combination of traces of acid and moisture. For example, ^{1}H-NMR spectroscopy revealed that dissolving pure samples of **4.1 - 4.6** in commercial $CDCl_3$ (which contains traces of water and HCl) results in partial or complete decomposition into the parent aldehyde and alkylurea,. In pure, acid-free $CDCl_3$ (obtained from treatment with Na_2SO_4 and K_2CO_3) and in DMSO-*d6* (which contains varying amounts of water but no acid) this problem does not exist.

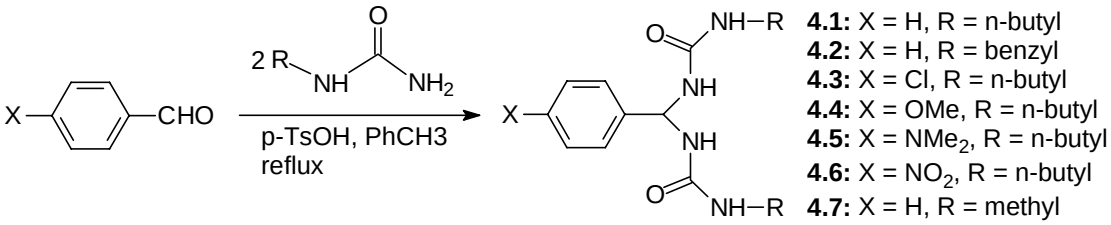

Scheme 4.1 Synthesis of geminal bis-urea compounds.

Other attempts (summarised in Scheme 4.2) to synthesise geminal bis-urea compounds with longer aliphatic tails (n-octyl, n-dodecyl) all failed. Using the diethylacetal of benzaldehyde instead of benzaldehyde gives the same results: inspection of the crude reaction mixture by ^{1}H-NMR spectroscopy showed that product had formed, but isolation was not successful. The same holds for the use of the trimethylsilyl-derivatives of mono-alkylureas. Although product was formed, all attempts to isolate it were unsuccessful.

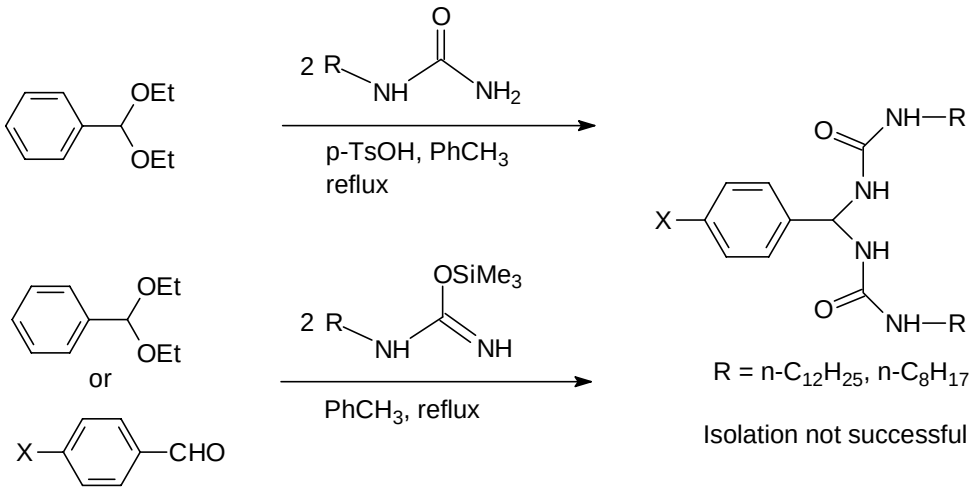

Scheme 4.2 Attempted syntheses of geminal bis-urea compounds.

4.3 Gelation of organic solvents

The gelating ability of geminal bis-urea compounds **4.1 – 4.6** for a range of organic solvents was examined (with the exception of **4.5**, which turned out to be too unstable with respect to hydrolysis) by dissolving ca. 10 mg of compound under heating in 1 ml of the desired solvent. The solubility of these compounds at room temperature is very poor in most solvents, chloroform being a notable exception. Upon cooling to room temperature, a gel, a precipitate or a clear solution was observed, depending on the solvent used. In the case of **4.1**, if gelation occurred, the concentration was gradually lowered until the ability to gelate had disappeared. The results are summarized in Table 4.1.

As can be seen, a gelator concentration range of 3 - 15 mM is typical, which range has also been found for other bis-urea compounds and many other organogelators.[2,5,7] Apparently these values represent a lower limit, at which the concentration of these aggregates is high enough and/or at which the size of the various aggregates in solution is large enough to sustain a 3D-network that retains the solvent, which eventually results in the formation of a gel.[2]

From Table 4.1 it is clear that **4.2** is the only ineffective gelator, which may be due to the fact that the butyl groups in the other compounds are much more flexible than the benzyl groups of **4.2**. This renders **4.2** an increased tendency to crystallize or to precipitate, rather than to form a gel. It is also clear that none of the compounds **4.1 - 4.6** gelate or precipitate in the tested protic solvents. NMR analysis revealed that in these solvents they easily decompose to an acetal and the parent monoalkylurea, which are both soluble in these solvents.

The gels given in Table 4.1 are stable for a period of at least three weeks at room temperature. In some cases (hexadecane, cyclohexane) the gels are very turbid and are destroyed easily by mechanical agitation, whereas in tetralin, *p*-xylene and toluene the gels are completely transparent and stable towards agitation. The gel from the methoxy-substituted compound **4.4** in tetralin is thixotropic, i.e. upon shaking, the gel loses its rigidity and becomes free flowing. Upon standing at rest for a few minutes the gel properties return completely. This process can be repeated many times (see also the previous chapter for another example of this behaviour).

Table 4.1 Gelation properties and critical gelator concentrations

Solvent	**Compound**				
	4.1	**4.2**	**4.3**	**4.4**	**4.6**
hexadecane	g (3)	p	g	p	i
cyclohexane	g (3)	p	g	g	g
toluene	g (5)	p	s	g	g
p-xylene	g (5)	p	s	g	g
tetralin	g (15)	p	s	g (t)	g
n-butylacetate	g (5)	p	s	p	p
1,2-dichloroethane	g (15)	p	s	g	p
chloroform	s	s	s	s	s
di-n-butylether	g (15)	p	g	g	p
acetonitrile	p	p	g	s	p
2-octanol	s (d)	s (d)	s (d)	s (d)	s (d)
2-propanol	s (d)	s (d)	s (d)	s (d)	s (d)
ethanol	s (d)	s (d)	s (d)	s (d)	s (d)
dimethylsulfoxide	s	s	s	s	s
cyclohexanone	p	s	s	s	p

Symbols: i: insoluble at solvent reflux temperature; p: precipitate; s: soluble at room temperature (solubility > 20 mg/ml); vs: viscous solution; t, thixotropic; d, decomposition. Values in parentheses denote the minimum concentration (mM) at which gelation still occurs.

In all cases gelation was found to be completely thermoreversible. Differential scanning calorimetry of a tetralin gel of **4.1** (80 mM) gave a very broad melting endotherm (T_{onset} = 90 °C, T_{max} = 119°C, T_{end} = 130 °C) with an enthalpy change of +65 kJ/mol. This enthalpy corresponds well with gelation enthalpies reported previously for bis-urea gelators in various solvents[5,6a] and is about twice as large as

the value that is found for breaking up large aggregates of mono-urea compounds in an apolar medium.[11] The broad temperature range of the melting process is indicative of a less cooperative phase transition.

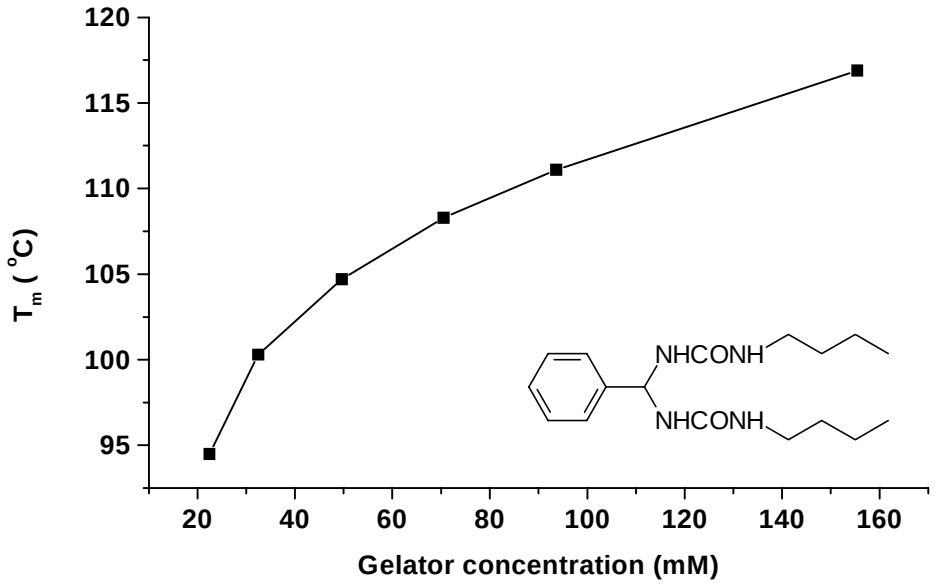

Figure 4.1 Melting points of tetralin gels of **4.1** as a function of concentration (determined by the dropping ball method).

The relation between gelator concentration and melting point of the gel was studied in tetralin by the dropping ball method (Figure 4.1).[12] The melting point determined by the dropping ball method lies ca. 10 °C below the maximum of the DSC melting endotherm, and therefore the evaluation of these data by a phase separation model or Schraders equation describing ideal solubility behaviour is not justified.[13,14,15] Furthermore, the dropping ball method signals a gradual weakening of the gel rather than a discrete phase transition, which is in complete agreement with the results from the DSC experiments.

Light microscopy shows that gels of **4.1** are birefringent, which is indicative of anisotropic properties, as was the case with previously reported bis-ureas,[3,6] but further structural details cannot be seen. Electron microscopy reveals that compound **4.1** is able to aggregate into long, intertwining bundles of fibers which are occasionally split up and fused with other fiber bundles (junction zones), thus showing that network does not result from purely mechanical contacts between the various fibers (Figure 4.2). The elongated shape of the fibers is most likely the result of a strongly anisotropic growth process, indicating that the intermolecular

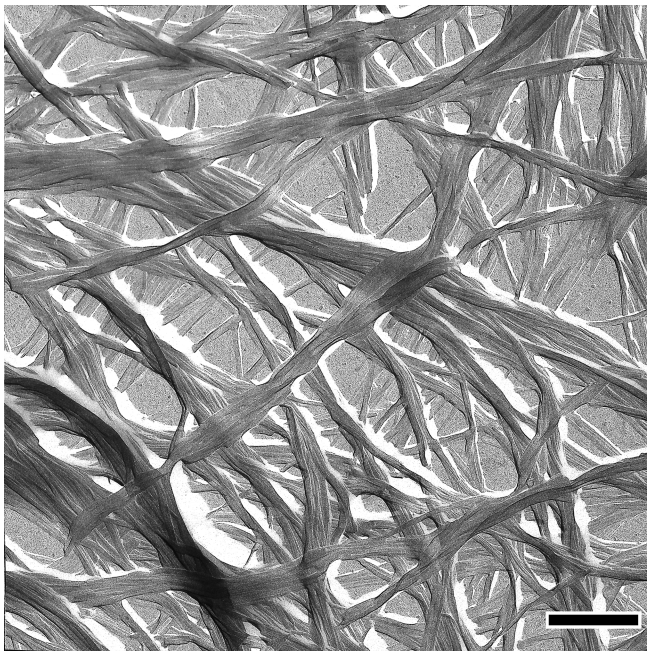

interactions are highly directional.[16] Electron microscopy of the various precipitates of **4.2** revealed that these precipitates consist of many relatively short crystallites.

Figure 4.2 Electron microscopy photograph of a tetralin gel of **4.1** (Pt shadowing, bar is 500 nm).

4.4 FT-IR experiments

The relation between gelating ability and intermolecular hydrogen bonding was studied by means of FT-IR spectroscopy, since the N-H stretch and the amide-I and amide-II bands of ureas generally show large shifts upon the formation of hydrogen bonds. When **4.1** is dissolved in 1,2-dichloroethane, we find that at low concentration (4.4 mM) there is a homogeneous solution and no gel is formed. This solution shows three absorptions at 3436 (N-H), 1690 (amide-I) and 1512 (amide-II) cm^{-1}, which are characteristic for non-hydrogen bonded urea groups (Table 4.2).[17] Increasing the concentration to 26.8 mM results in the formation of a gel, and the IR spectrum of this gel showed that the urea adsorption bands are shifted towards 3306, 1634 and 1562 cm^{-1}. These spectral shifts are characteristic for the presence of hydrogen bonded urea groups, and apparently formation of a gel is accompanied by the formation of intermolecular hydrogen bonds between the urea groups. The absorptions for solid **4.1** (nujol mull) are in close agreement with these data (3343, 1632, 1561 cm^{-1}, respectively), indicating that in the solid state hydrogen bonding also occurs.

Although **4.1** does not form gels in chloroform, it was found that aggregates are formed in this solvent (*vide infra*). The FT-IR spectrum of a homogeneous solution of **4.1** in chloroform at low concentration shows strong absorptions for the urea groups at 3443 (N-H), 1667 (amide-I) and 1523 (amide-II) cm^{-1}, which corresponds very well with values reported for *N,N'*-dialkylureas in the same solvent.[18] Increasing the

concentration of **4.1** to 47.7 mM causes a shift of these absorptions towards 3340, 1639, and 1560 cm^{-1} respectively (Table 4.2). These concentration dependent spectral shifts are again indicative of the formation of aggregates stabilized by intermolecular hydrogen bonds between the urea groups.[7b,5b]

Table 4.2 FT-IR data for **4.1** in the solid state, in solution and in the gel state*

	Absorptions (cm^{-1})		
Solvent and concentration	NH-stretch	Amide-I	Amide-II
$CHCl_3$, 2.8 mM (sol)	3443	1667	1523
$ClCH_2CH_2Cl$, 4.4 mM (sol)	3436	1690	1512
$CHCl_3$, 47.7 mM (sol)	3340	1639	1560
$ClCH_2CH_2Cl$, 26.8 mM (gel)	3306	1634	1562
nujol mull	3343	1632	1561

* All spectra are recorded at room temperature.

4.5 Molecular modeling

Molecular modeling is a powerful tool with which an insight can be obtained into the interaction potential surface of molecules and into their possible modes of aggregation, but for many known gelators the use of molecular modeling is complicated by the large degree of conformational freedom of the compounds. In order to reduce the conformational space to a minimum, geminal bis-urea **4.7** was chosen as a model compound for the molecular modeling experiments. The conformational space of **4.7** is formed by the three dihedrals ϕ1, ϕ2, and ϕ3 of the bonds connecting the urea moieties and the phenyl group with the geminal carbon atom (Figure 4.3).

A conformational search using the CHARMm force field as implemented in Quanta97 was carried out by systematic variation of ϕ2 and ϕ3 whereas no restrictions were applied to ϕ1.[19] Only one stable conformation (**4.7a**) was identified by this conformational search, which for symmetry reasons results in two global energy minima on the potential energy surface formed by the dihedral angles ϕ2 and ϕ3

(Figure 4.4). In the minimum energy conformation a single intramolecular hydrogen bond is present. The rotation of the urea groups around ϕ2 and ϕ3 is marked by two saddle points, which are 6.6 kcal/mol and 8.0 kcal/mol higher in energy (**4.7b**, **4.7c**, Figure 4.4).

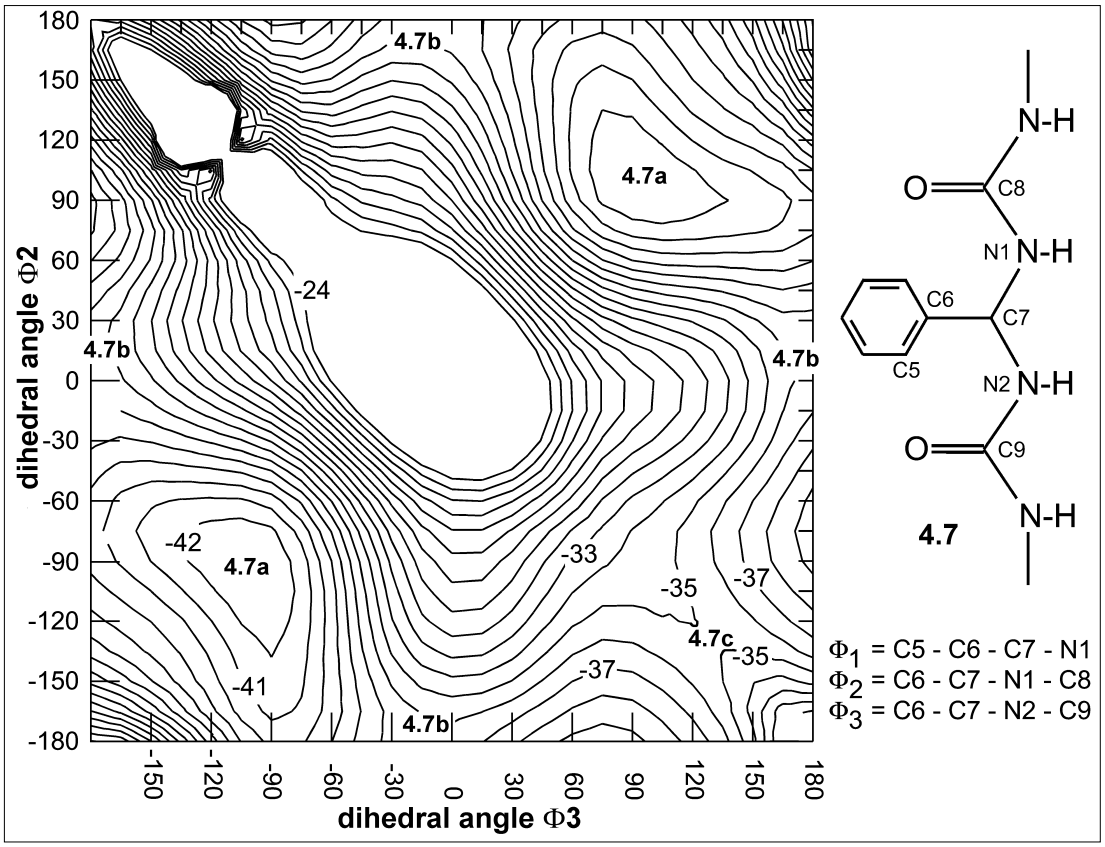

Figure 4.3 Conformational space and potential energy surface of 4.7.

The interaction potential surfaces of **4.7a-c** were explored by calculating the interaction energy between a molecule of **4.7** located at the center of a cubic box with a second molecule of **4.7** while systematically varying the Euler angles of rotation and repeating this procedure at each point of a cubic box spaced by 0.5 Å in each direction. The interaction potential surfaces of the conformers **4.7a** and **4.7b** do not show preferential sites for complementary hydrogen-bond interactions with a second molecule. This is in large contrast with **4.7c**, which has a highly anisotropic interaction potential surface, with the most favourable sites of interaction being located on the axes along the urea carbonyl bonds (Figure 4.5). Similar results have been obtained for bis-ureas based on 1,2-diaminobenzene and 1,2-diaminocyclohexane (see also Chapter 3).[7b]

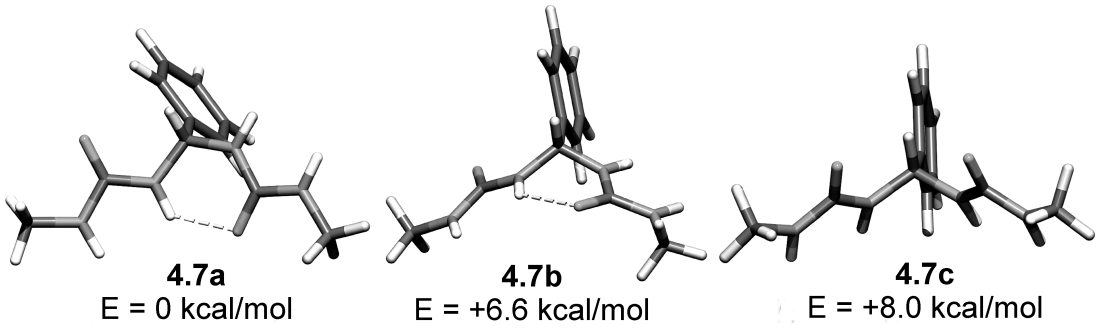

Figure 4.4 Minimum energy and saddle point conformations of **4.7**.

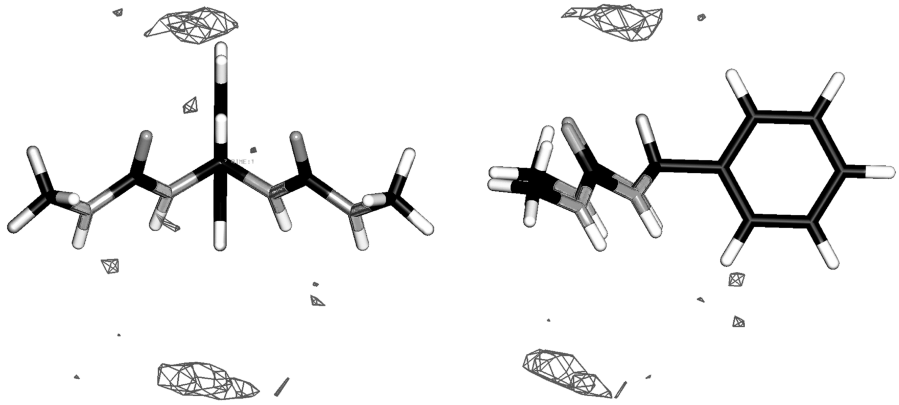

Figure 4.5 Interaction potential surface of **4.7c**.

One-dimensional aggregates of **4.7** can be constructed by applying the appropriate symmetry operations to the various conformers: translation (P1), screw axis ($P2_1$), glide plane (Pa) or inversion (P-1).[20] When these operations are carried out along an axis that runs through the most favourable site(s) of interaction, which can be obtained from the interaction potential surface, one can expect that the most stable 1D-aggregates will be formed.

When we are dealing with a conformer of **4.7** that has an *antiparallel* (*a*-) orientation of the urea groups, it is possible to build aggregates from this conformer through the application of a translation (*a*-P1), glide plane (*a*-Pa) or inversion (*a*-P-1) operation. Conformers of **4.7** that have a *parallel* (*p*-) orientation of the urea fragments can be used to build aggregates through the application of a translation (*p*-P1), screw axis (*p*-$P2_1$) or glide plane (*p*-Pa) operation (depicted in Figure 4.6a).

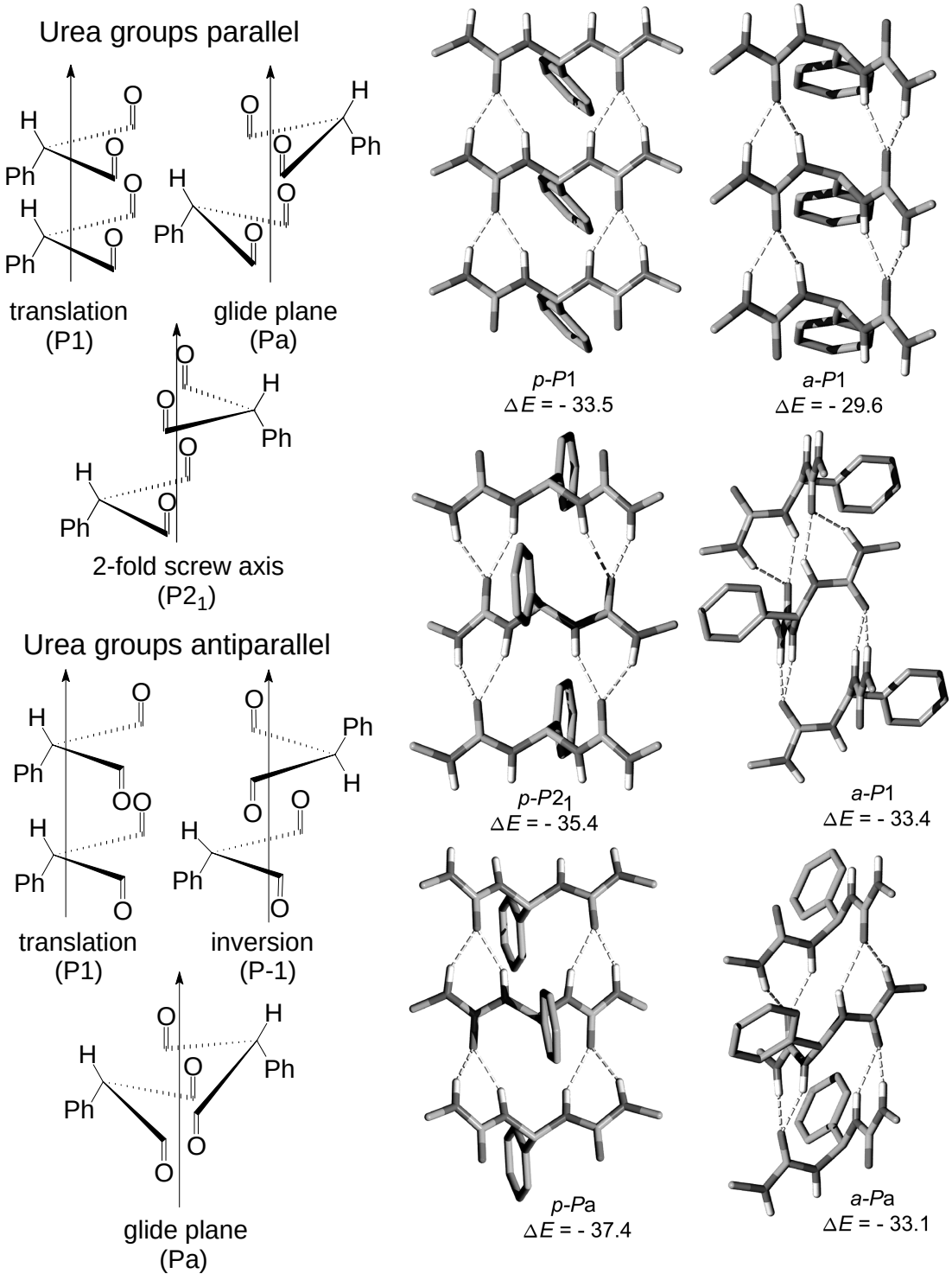

Figure 4.6. a) Left: schematic drawings of symmetry restricted aggregates of **4.7**. For reasons of clarity the hydrogen bonding direction of the urea groups is indicated by the carbonyl groups only. b) Right: fragments of symmetry-restricted aggregates of **4.7** obtained by molecular modeling. Energies (kcal/mol) are per molecule relative to conformer **4.7a**.

The structures and stabilities of all these six aggregate forms were investigated by means of molecular mechanics calculations (figure 4.6b). Although no specific sites of interaction could be obtained for conformers **4.7a** and **4.7b** through the computation of the interaction potential surface (*vide supra*) it was found that they do give stable one-dimensional aggregates, all with an antiparallel orientation of the urea groups. The use of conformer **4.7c** leads to aggregates with the urea groups oriented in a parallel fashion. The loss of the intramolecular hydrogen bond in the two conformers **4.7a,b** is compensated by the formation of four intermolecular hydrogen bonds between adjacent molecules. It was found that in all these aggregates every urea group participates completely in hydrogen bonding with an adjacent molecule.

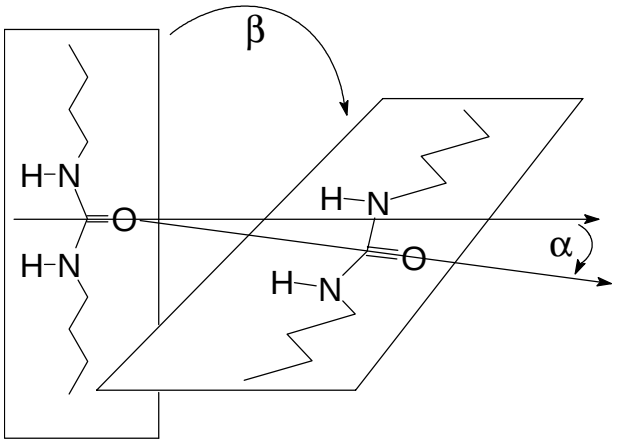

Figure 4.7 The colinearity angle α and the angle β between the two planes in which the successive hydrogen bonded urea fragments lie.

The structures of the calculated hydrogen bonded networks are in general in good agreement with what is found for various mono-urea derivatives in the solid state. For the translation aggregates *p*-P1 and *a*-P1, the repeating distances that give the lowest aggregate energies are 4.5 - 4.6 Å, values that are in excellent agreement with previously reported X-ray data.[21] The other aggregates contain two molecules per unit cell and give repeating distances in the range of 8.8 - 9.0 Å, which are also in good agreement with literature reports.[7b,21] A distinct feature of urea compounds is that in crystal structures the urea groups tend to form colinear and coplanar hydrogen bonded arrays (Figure 4.7, see also Chapter 1).[20,21] Within the *a*-Pa and *a*-P-1 aggregates, however, the hydrogen bonded arrays deviate substantially from colinearity and coplanarity, with $\alpha = 90^{o}$ and $\beta = 28^{o}$ for *a*-Pa and $\alpha = 95^{o}$ and $\beta = 27^{o}$ for *a*-P-1. Therefore these aggregates are less likely to occur. In the aggregates with *a*-P1, *p*-P1, *p*-$P2_1$ and *p*-Pa symmetry the urea groups form indeed (almost) colinear and coplanar hydrogen bonded arrays. Of these aggregates, the ones with *p*-$P2_1$ and *p*-Pa symmetry are the most stable, indicating that an alternating orientation of successive molecules is more favourable.[21,22]

4.6 NMR experiments

In general, NMR techniques can give a great deal of information with respect to, for example, self-assembly processes in solution. Especially the use of NOESY experiments may provide insight in how molecules are oriented with respect to one another in an aggregated state. It was found that the geminal bis-urea compounds do not form gels in chloroform and are soluble up to a concentration of at least 78.0 mM. Nevertheless, concentration dependent infrared measurements showed that these compounds nevertheless do aggregate in this solvent (*vide supra*). We therefore studied the aggregation behaviour of these compounds in chloroform in more detail by using ^{1}H- and ^{13}C-NMR techniques. ^{1}H-NMR measurements of compound **4.1** in $CDCl_3$ showed that the spectra are extremely sensitive to changes in concentration and temperature. Concentration dependent measurements revealed that at low concentrations (< 0.62 mM) the ^{1}H-NMR spectrum does not change significantly, but

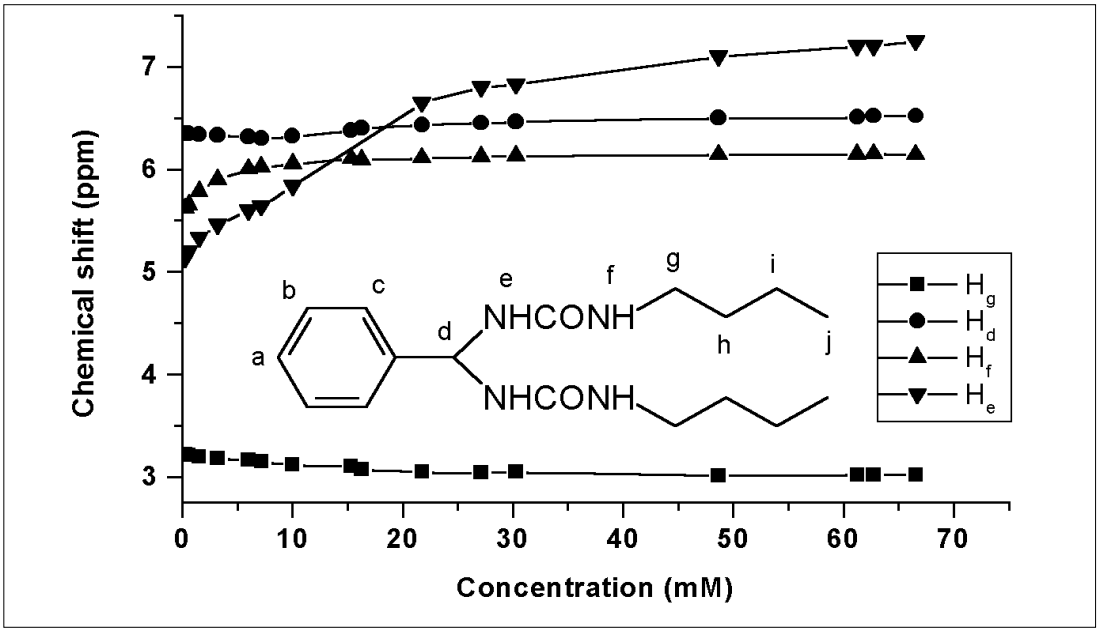

Figure 4.8 Concentration dependent ^{1}H-NMR shifts of **4.1** in $CDCl_3$ at 25 ^{o}C.

an increase of the concentration resulted in clear downfield shifts of the spectral positions of the NH protons and an upfield shift of the spectral positions of the α-CH_2 protons, until at higher concentration a plateau is reached (Figure 4.8). Apparently, at low concentration **4.1** is mainly present as a monomer, whereas at higher concentration the equilibrium is shifted in favour of the aggregate.[23] These results are in excellent agreement with the FT-IR data. The data in Figure 4.8 could not be fitted

in a model involving only the formation of dimers, thus suggesting that higher aggregates rather than dimers are involved.[24] The formation of higher aggregates is also confirmed by NOESY experiments (*vide infra*).

The ^{1}H-NMR spectra of **4.1** in $CDCl_3$ are very sensitive to changes in temperature. Increasing the temperature for a concentrated solution (47.7 mM) of **4.1** causes an upfield shift of the spectral positions of the NH protons and a downfield shift of the α-CH_2 protons, indicating a return to mainly monomeric species in solution. Decreasing the temperature causes the opposite effect, and is accompanied by line-broadening of the spectra. Obviously, at higher concentrations the degree of aggregation is strongly dependent on the temperature.

At low concentrations a change of the temperature has a different effect (Figure 4.9). At 20 ^{o}C and a concentration of 1.6 mM the NH(e) and NH(f) signals are broad singlets but when the temperature is raised to 50 °C, the NH(e) signal becomes a well resolved doublet. On the other hand, decreasing the temperature results in a broadening of only the NH signals, until at –10 °C they completely disappear, but at a temperature of –30 °C four new signals appear (at 5.09, 5.61, 6.03 and 6.87 ppm, respectively, Figure 4.9). Apparently, at –30 ^{o}C and lower all four NH protons are non-equivalent, indicating that rotation around ϕ1 and ϕ2 (Figure 4.3) has become slow on the NMR time scale. These results are in excellent agreement with the molecular modeling calculations, which indicate that the minimum energy conformation lacks an element of symmetry and that this conformation is stabilized by the presence of a single intramolecular hydrogen bond. Apparently, at room temperature this intramolecular hydrogen bond becomes weak enough so that rotation around ϕ1 and ϕ2 becomes fast on the NMR time scale and consequently the NH protons are observed as two time-averaged signals.

Interestingly, the coupling pattern of the urea NH protons indicates that for the monomeric species the position of the NH(e) proton is upfield relative to the position of NH(f). This is confirmed by 2D NOESY (vide infra) and COSY experiments. As it is shown in Figure 4.8, upon aggregation a large downfield shift of NH(e) of 1.5 ppm is observed (going from 0.31 to 60.2 mM in $CDCl_3$), whereas the other signals shift only by 0.2-0.5 ppm. The high-field position of the NH(e) signal relative to the NH(f) signal at low concentration and high temperature (Figure 4.9) is quite remarkable and counterintuitive, since one would have expected it the other way around, based on substituent effects. ^{1}H-NMR experiments with the model compound *N*-benzyl-*N'*-

octylurea showed that in this compound this is indeed the case: the signal from the NH next to the benzylic CH_2 is indeed shifted to a lower field than the signal from the NH next to the aliphatic CH_2. Most likely, the anomalous upfield position of the

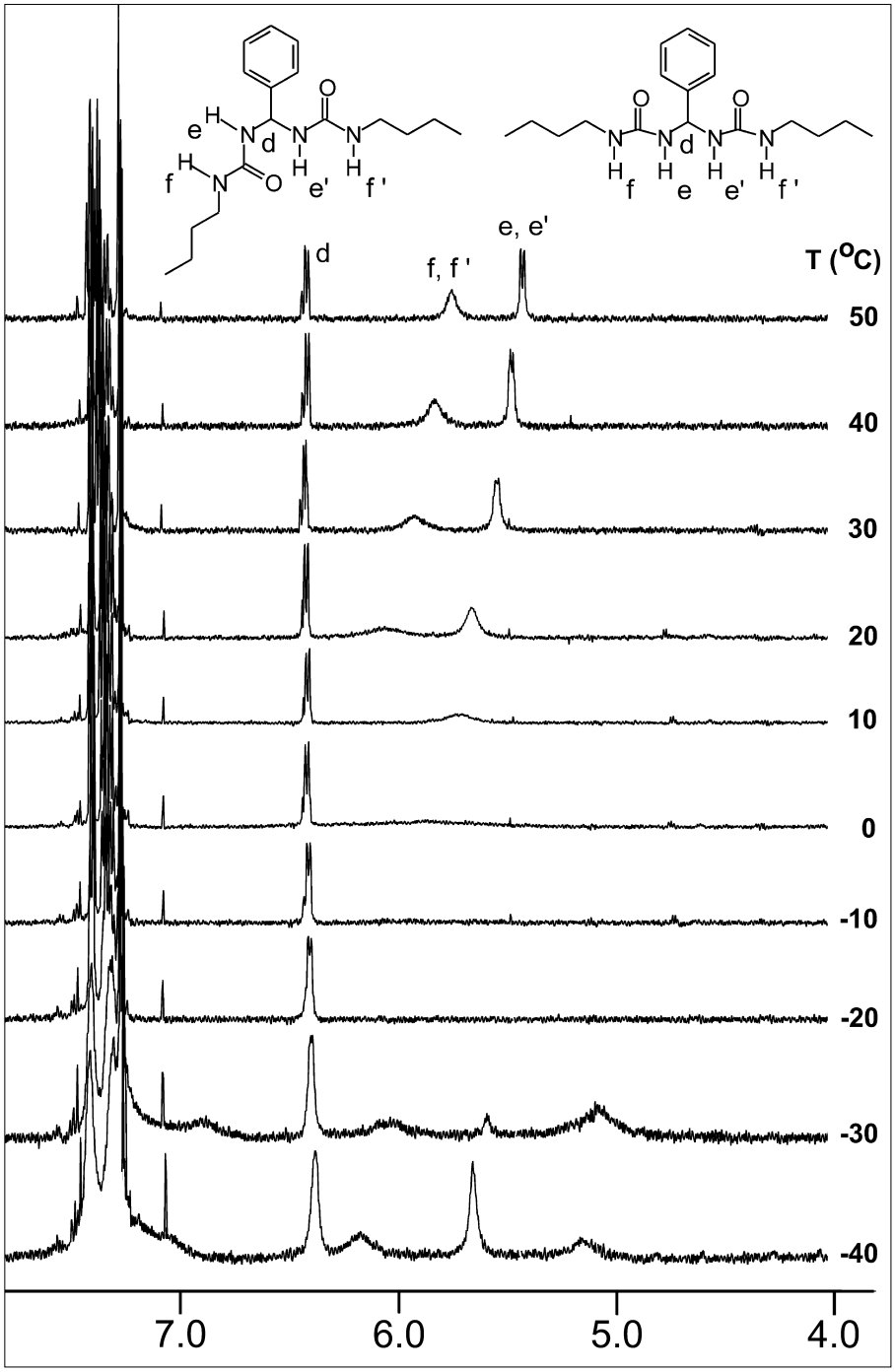

Figure 4.9 Temperature dependent ^{1}H-NMR spectrum of a 1.6 mM solution of **4.1** in $CDCl_3$.

which showed that for the minimum energy conformation **4.7a** one of the NH(e) protons is indeed located in the shielding region, and apparently also compound **4.1** exists predominantly in the most stable intramolecular hydrogen bonded form both at low as well as at higher temperatures. Since upon aggregate formation a significant conformational change must take place, the NH(e) proton is no longer to be found in the shielding region of the phenyl group, and consequently for the aggregated species present at high concentration the signals of the NH protons return to their 'normal' spectral positions as one would have expected, based on substituent effects and the formation of hydrogen bonded urea species. More support for this idea comes from the data obtained from ^{1}H-NMR spectra with DMSO-*d6* as a solvent. In DMSO-*d6* no aggregation takes place and it also is not likely that intramolecular hydrogen bonding occurs due to its strongly hydrogen bond accepting character, which is known to disrupt inter- and intramolecular solute hydrogen bonds. In this solvent, it is found that for all compounds **4.1 - 4.6** the signal for the NH(e) proton lies downfield with respect to the signal for NH(f), exactly as expected on the basis of substituent effects.

In order to obtain more information about the structure of these aggregates, two NOESY-experiments were carried out with **4.1** in $CDCl_3$ at different temperatures and concentrations. At 50°C and a concentration of 4.0 mM, the only cross peaks observed are the ones from nearest neighbour contacts, so it can be concluded that there is (almost) exclusively non-aggregated **4.1** in solution. Increasing the concentration to 27.2 mM at 25°C results in a number of additional NOE cross peaks, especially between the phenyl and butyl segments of the molecule (Figure 4.10). It was observed that all NOE enhancements in the aggregated state are negative, whereas they are all positive in the non-aggregated state. This indicates that at this concentration and temperature the majority of the formed aggregates have a molecularweight of at least 1500 or higher, which means that these aggregates consist of at least 6 monomeric units.[25] Apparently, the additional NOE interactions observed at high concentration correspond to intermolecular close contacts only present in the aggregate of **4.1**.

On the basis of the additional NOE interactions it is evident that there must be aggregates present with $P2_1$, Pa or P-1 symmetry (Figure 4.6), since only in these aggregates there will be NOE interactions between protons of the phenyl and butyl groups (Figure 4.11). In a strict sense it is not possible to exclude polymorphism (the simultaneous existence of different aggregate symmetries in the same solution), just as it is not possible to exclude the presence of aggregates with P1 symmetry on the basis of these NOESY experiments alone. However, on the basis of the simplicity of

the observed ^{1}H- and especially ^{13}C-NMR spectra (*vide infra*) it is reasonable to assume that polymorphism is highly unlikely in this situation.

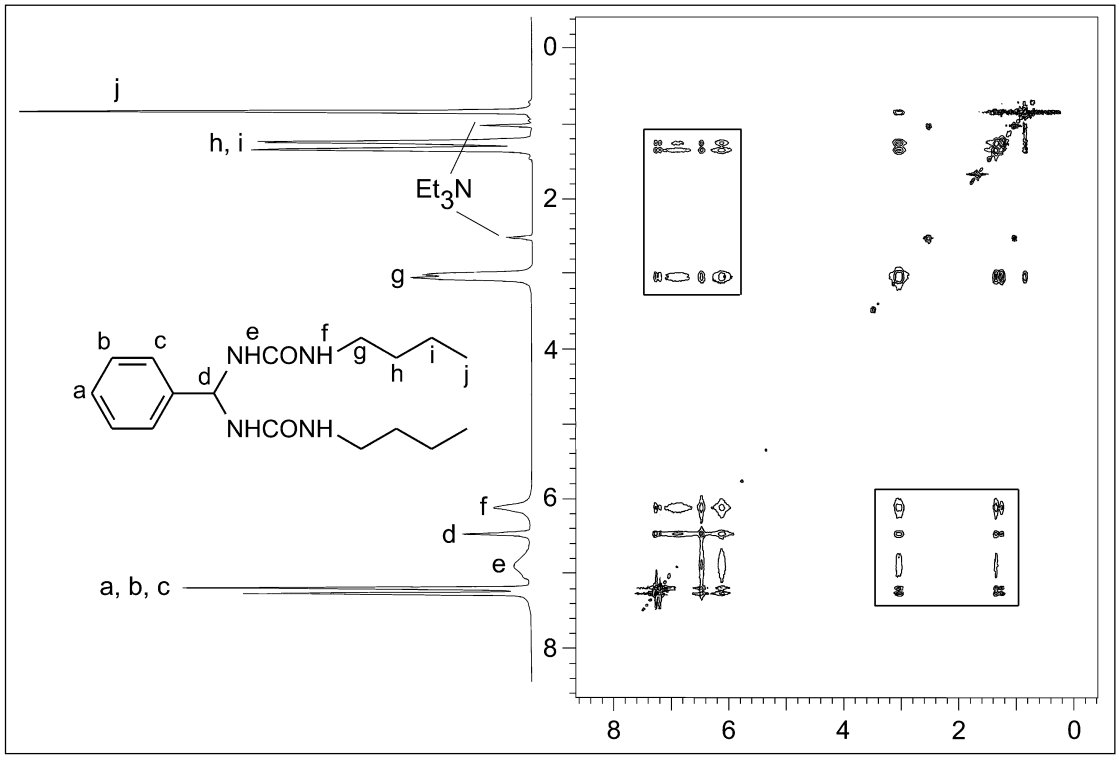

Figure 4.10 NOESY spectrum of **4.1** at a concentration of 27.2 mM in $CDCl_3$.

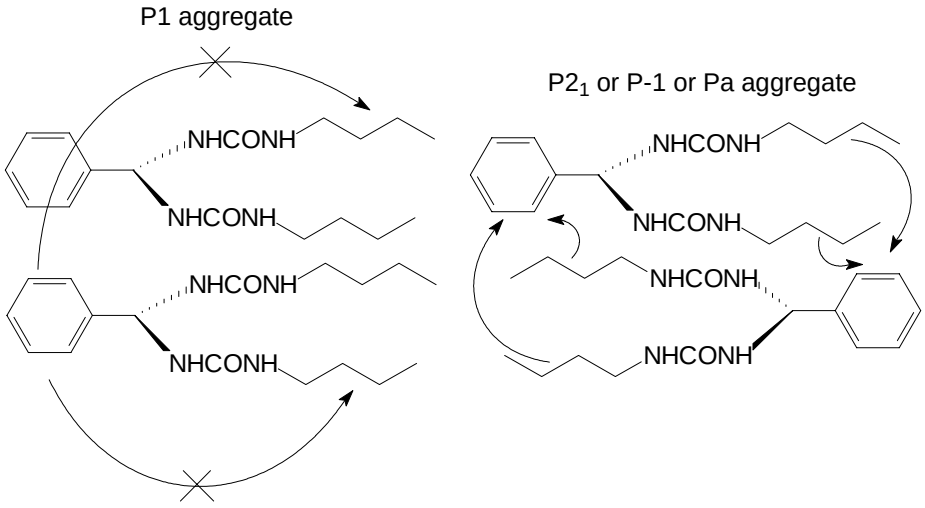

Figure 4.11 Explanation of NOE interactions between adjacent molecules of **4.1**.

Since the FT-IR spectroscopy results showed that hydrogen bonding also occurs in the solid state (vide supra) ^{1}H-MAS and ^{13}C-CP/MAS NMR experiments were carried out in order to establish a relationship between the aggregated species in solution ($CDCl_3$), in the gel-state ([D_8]toluene), and in the solid state.[26] In general it was found that attempts to measure ^{1}H-NMR spectra of gels are not successful owing to excessive dipolar broadening and ^{1}H MAS NMR of both the gel and the solid state gave complex and highly broadened spectra, most likely due to dipolar interactions and spin diffusion. However, the ^{13}C-CP/MAS NMR spectra are of a much better quality (Figure 4.12), giving nicely resolved signals of both the solid state and the gel state, although the ^{13}C-NMR spectrum of the latter has a poor S/N ratio, due to limited experiment time. A comparison of **4.1** at low concentration in DMSO-*d6* (Figure 4.12a), at low concentration in $CDCl_3$ (Figure 4.12b), at high concentration in $CDCl_3$ (Figure 4.12c), in the solid state (Figure 4.12d), and the gel state in toluene-*d8* (Figure 4.12e) reveals that the changes in the spectral positions of the various carbon atoms are less dramatic than for the corresponding proton spectral positions in the ^{1}H-NMR, which is not unreasonable since one would also expect that aggregation phenomena have a more pronounced effect on ^{1}H shifts than on those of ^{13}C.

It was observed that at both low and high concentration of **4.1** in $CDCl_3$ (Figure 4.12b and 4.12c) the carbonyl signal (p) has about the same position, even though at high concentration aggregates are formed. The fact that upon aggregation the carbonyl spectral position is shifted by not more than 0.1 ppm is most likely due to the fact that at low concentration intramolecular hydrogen bonding takes place, combined with additional weak hydrogen bonding between the solvent (H-bond donor) and the solute (both H-bond acceptor and donor). Apparently these combined interactions have the same effect upon the chemical shift as aggregation. In the gel and in the solid state the same spectral positions are found for the carbonyl signal, indicating again that in the solid state hydrogen bonding also occurs. In DMSO-*d6* (H-bond acceptor) an upfield shift of 1.3 ppm is observed. Doubling of the signals for the carbonyl carbon was not observed in solution or in the solid and gel states, suggesting that both carbonyls are equivalent, although in solution there is of course always the possibility of a fast exchange (*vide supra*). If the two carbonyls of **4.1** are equivalent in the aggregate and in the gel state, then the only possible aggregate symmetries are *p*-P2_1 and *p*-Pa (Figures 4.5, 4.6).For the quaternary phenyl carbon (n) a different behaviour is observed. It shifts from 142.8 ppm in DMSO-*d6* (Figure 4.12a) to 139.9 ppm in $CDCl_3$ at low concentration (Figure 4.12b), which results mainly from going from a conformation with no intra- or intermolecular hydrogen bond (in DMSO-*d6*) to the

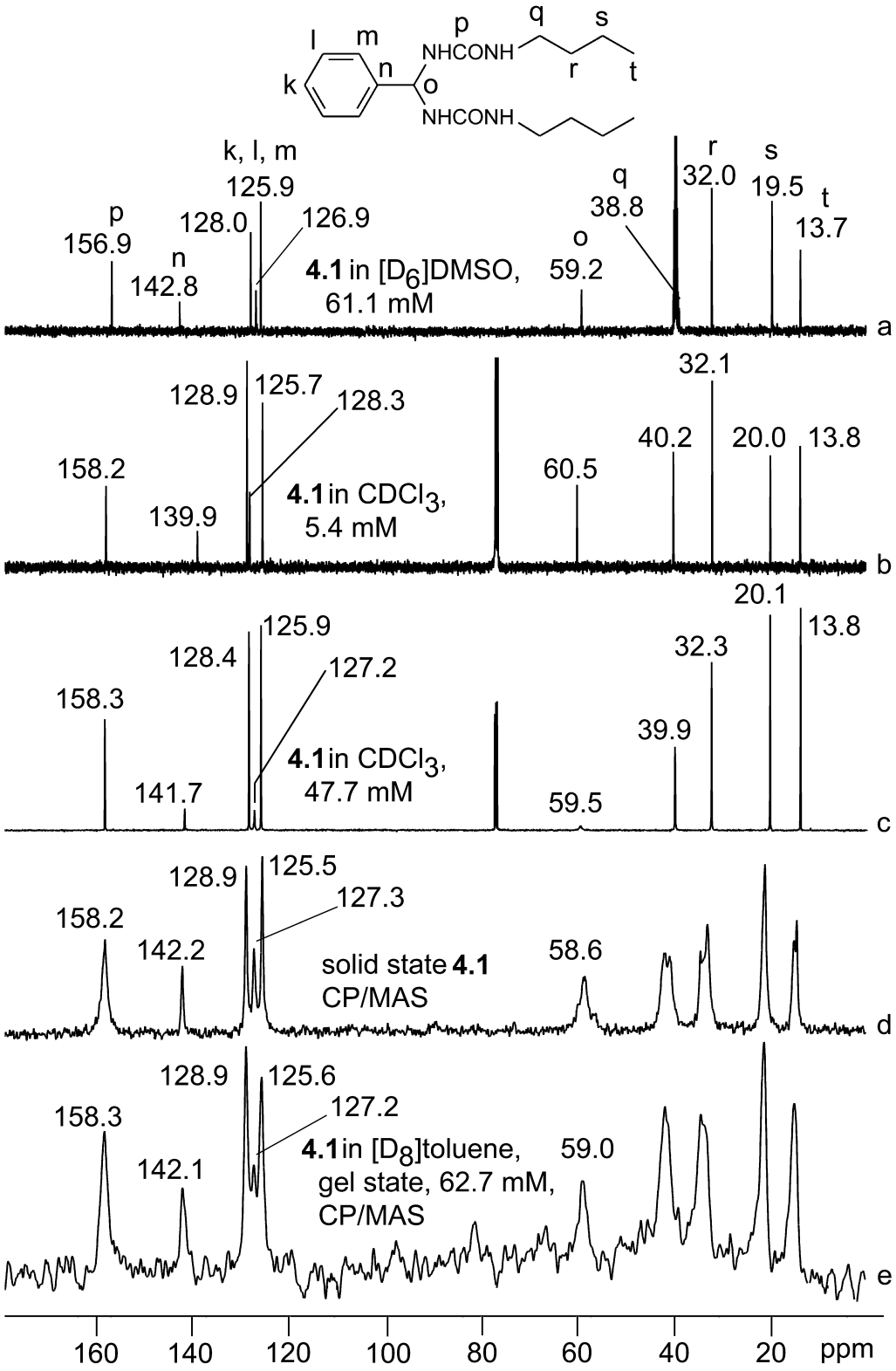

Figure 4.12 Comparison of solution ^{13}C-NMR data (a: 61.1 mM in DMSO-*d6*; b: 5.4 mM in $CDCl_3$; c: 47.7 mM in $CDCl_3$) of **4.1** with ^{13}C-NMR CP/MAS data of the solid state (d) and the gel state (e: 62.7 mM in [D_8]toluene) of **4.1.**

formation of an intramolecular hydrogen bond and hence to a change of the conformation of **4.1**. As soon as aggregation takes place (Figures 4.12c and 4.12e), the signal of this quaternary carbon atom (n) shifts downfield again. In the solid state virtually the same position is found as in the gel state (Figure 4.12d). Furthermore, upon aggregate formation in $CDCl_3$ (Figure 4.12c) the signal of the geminal carbon atom (o) shows a large line broadening. This points to a fast relaxation of this carbon atom, probably due to the fact that upon aggregate formation the two urea dipoles are locked.

In general the chemical shifts in the solid state, gel state, and high concentration in $CDCl_3$ are almost the same, indicating that **4.1** has the same conformation in these different states. In the solid state the signals of the butyl carbons of **4.1** are clearly split, whereas this is not the case for the phenyl carbons. This means that in the solid state all the phenyls are equivalent, but that there are two non-equivalent butyls present. If this splitting of butyl signals also holds for the gel state whereas the phenyl signals do not split, then that would be strong evidence for an aggregate with Pa-type of symmetry (Figures 4.5, 4.6), since in an aggregate with this symmetry the two butyl groups of **4.1** are inequivalent. The same is probably true in the gel state, but given the signals as they are (poor quality spectrum) this cannot be considered hard evidence. Another reason for the splitting of the signals may be found in the packing of the linear aggregates in the solid state and the gel state, which gives rise to secondary interactions that are of course not present in solution.

4.7 Conclusions

It has been demonstrated that geminal bis-urea compounds are effective gelators for various organic solvents, showing that the concept of strong unidirectional intermolecular interactions is very useful for the design of new organogelators. The gels formed by these geminal bis-urea compounds have much in common with gels from cyclic bis-urea gelators previously reported by our group: gel formation already takes place at very low concentrations (typically less then 15 mM) in a variety of organic solvents, and is completely thermoreversible with melting temperatures up to 115 ^{o}C. Electron microscopy showed that gel formation by the bis-urea gelling agents is due to the formation of long, intertwined fibers having widths of 30-300 nm and lengths up to 40 μm, whereas FT-IR and ^{1}H-NMR experiments in chloroform and 1,2-dichloroethane solutions showed that aggregation of these geminal bis-urea

compounds is accompanied by formation of intermolecular hydrogen bonds between the urea groups.

The relationship between molecular structure, aggregation ability and structure was studied in more detail by molecular modeling and NMR spectroscopy. Molecular modeling revealed that these geminal bis-urea compounds can form highly stable one-dimensional aggregates, which are stabilized by four hydrogen bonds between urea groups of adjacent molecules within the aggregate. Most interestingly, the modeling experiments also indicate that for the minimum energy conformation of the monomer the urea moieties do not have the proper orientation for the formation of stable one-dimensional aggregates. Upon aggregation, however, a conformational change takes place that involves rotation of the urea moieties to a coplanar orientation, thereby exposing all hydrogen bonding sites along one common direction. NMR experiments showed that such a conformational change indeed takes place upon the formation of hydrogen bonded aggregates, and, moreover, that the conformation in the aggregate and the gel state is the same.

A symmetry analysis of possible one dimensional aggregate structures of bis-urea compounds showed that in principle a number of aggregate structures are possible, which are all stabilized by the maximum number of hydrogen bonds between adjacent molecules. The relative stabilities of the possible aggregate structures were investigated by molecular modeling and these studies indicate that aggregates with either *p*-$P2_1$ or *p*-Pa symmetry are favoured over others. The results of the NOESY-NMR experiments nicely agree with the molecular modeling calculations: the observed intermolecular close contacts between the phenyl and butyl moieties of the geminal bis-urea compound unambiguously show the presence of aggregates with either *p*-$P2_1$ or *p*-Pa symmetry, but the presence of aggregates with P1 (translation) symmetry cannot be excluded.

These studies clearly show that molecular modeling and solution NMR studies of aggregation of organic gelling agents in combination with solid state NMR studies can give valuable insights into gel formation and gel structure. Although at present polymorphism in solution and in gels of geminal bis-ureas cannot be excluded, the NMR studies point to the presence of exclusively one kind of aggregate.[27]

4.8 Experimental Section

Molecular Modeling

Molecular modeling calculations were carried out using the CHARMm 23 force field as implemented in Quanta97/CHARMm, a product of Molecular Simulations Inc., San Diego, USA. All calculations were carried out in the gas phase with a dielectric constant of 1. For the nonbonding interactions a cut-off radius of 15 Å was used with a switch function working from 11 to 14 Å. Template charges were used and all energy terms were included, with the exception of an explicit hydrogen bonding term.

For the calculation of interaction maps (docking experiments) one molecule (substrate) of **4.7** was placed at the center of a cube (15 x 15 x 15 $Å^3$), with grid points spaced at 0.5 Å. A second molecule (probe) was placed on a grid point and allowed to rotate with 30^o increments around the Euler angles, whereby the interaction energy with the substrate was computed for each rotation. This procedure was repeated for each grid point, after which the interaction map could be constructed.

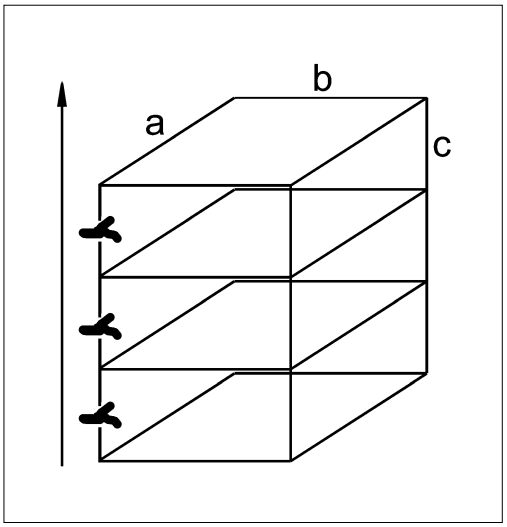

For calculations of the possible 1D-aggregates the crystal modeling facility of Quanta97/CHARMm was used, with the application of periodic boundary conditions. One conformer of **4.7** is placed in a tetragonal unit cell (a = b ≠ c) in such a way that the C=O bonds of the urea groups are more or less (anti)parallel with one of the crystallographic axes (e.g. c) . Two sides of the box (a, b) are kept at a constant size of 50 Å, which is much larger than the cutoff radius for nonbonded interactions in CHARMm. In this way it is certain that no interaction with neighbouring molecules is taken into account in these directions. The third side of the box, corresponding with the applied symmetry operation, is kept much smaller and is systematically varied. By doing so we only include intermolecular interaction along the **c**-axis and thus 1D aggregation. The chosen length of this side of the box is varied from 4.2 - 5.0 Å when there is one molecule per unit cell (translational symmetries *p*-P1 and *a*-P1), or from 8.4 - 9.4 Å when there are two molecules per unit cell (all other symmetries), thus yielding the minimum energy distance and optimal aggregate structure.

Electron Microscopy

For electron microscopy a piece of the gel was deposited on a formvar/carbon coated copper grid (400 mesh) and removed after one minute, leaving some small patches of the gel on the grid. After drying at low pressure ($<10^{-5}$ Torr) the specimen was shadowed at an angle of 45^{o} with platinum. The specimen was examined in a JEOL 1200 EX transmission electron microscope operating at 80 kV. In studying the specimen, we first searched for patches of the gel to be sure that the observed structures originate from the gel. Micrographs were taken from structures at the periphery of the gel patches because here the fibers are deposited in a layer thin enough to be observed by transmission electron microscopy.

NMR experiments

Routine NMR spectra were recorded on a Varian VXR-300 spectrometer. All other experiments were performed on a Varian VXR-500 MHz spectrometer, with the exception of MAS-experiments, which were carried out with a Varian Unity 400 WB NMR spectrometer operating at 400 and 100 MHz for ^{1}H and ^{13}C, respectively. Chemical shifts are denoted in δ units (ppm) relative to $CHCl_3$ (^{1}H: δ = 7.27 ppm, ^{13}C: δ = 77.0 ppm) or DMSO (^{1}H: δ = 2.49 ppm, ^{13}C: δ = 39.5 ppm). 2D NOESY experiments were carried out with the following parameters: spectral width 4500 Hz; 16 transients for each FID; 512 t_1 increments and a 2024 x 2024 data matrix; a mixing time t_m = 0.6 s was used; a $\pi/2$ shifted sine-squared weighting function was applied prior to Fourier transformation.

For solid state experiments, a Jakobsen-design probe head was used in combination with a Sørensen heating apparatus and a Varian rotor speed control unit. The 5 mm ZrO_2 spinners were spun under the magic angle wi th speeds of 8.9 kHz (for solids) and at 1.8 kHz (for gels) at 30^{o}C. ^{13}C spectra were recorded after careful molding using a recycle time of 5 s of more and gated high power decoupling (GHPD) during acquisition. Usually, the accumulation of 3000-6000 transients resulted in ^{13}C spectra with appropriate signal to noise ratios. The solid state spectra in the gel state were carried out using deuterated co-solvents in order to suppress additional solvent signals and allow the recording of ^{2}D ^{1}H-^{1}H spectra. The deuterium signal was used for locking by tuning the *X*-channel on the deuterium frequency during 2D experiments.

Gelation experiments

In a typical gelation experiment a weighed amount (ca. 10 mg) of the bis-urea compound and 1 ml of the solvent were put in a GC-vial, after which the vial was

tightly sealed with a thin teflon disk and a screw cap. The vial was then heated with shaking until all the solid material had dissolved. The solution was set aside and allowed to cool to room temperature. Gelation was considered to have occurred when a homogeneous substance was obtained, which exhibited no gravitational flow.

For the determination of melting points of the gels a steel ball (150 mg) was placed on top of a gel, after which the vial was sealed. A series of these samples was placed in a stirred oil bath that was slowly heated (typically 2 - 4 ^{o}C min^{-1}), while the positions of the steel balls were observed and the temperature was simultaneously monitored with the aid of a thermocouple in one of the vials. The temperature at which the steel ball had reached the bottom of the vial was considered to be the melting point of a sample.[12]

All compounds used (benzaldehyde, *p*-chlorobenzaldehyde, *p*-methoxybenzaldehyde, *p*-nitrobenzaldehyde, dimethylaminobenzaldehyde, butylurea, benzylurea) are commercially available (Aldrich, ACROS) and were used without further purification. Toluene and ether were distilled from sodium prior to use. Dichloromethane was distilled from P_2O_5 prior to use. $CDCl_3$ (Aldrich) was dried and freed from traces of acid over Na_2SO_4/K_2CO_3 and kept basic with some triethylamine in order to prevent geminal bisurea **4.1** from decomposing during the NMR experiments. DMSO-*d6* (Aldrich) was used as received and stored over molsieves.

Synthesis of 1-butyl-3-[(3-butylureido)phenylmethyl]urea (4.1).
Benzaldehyde (2.03 g, 19.1 mmol) and *n*-butylurea (4.44 g, 38.2 mmol) were suspended in 125 ml of toluene. A few crystals of p-TsOH were added and the solution was refluxed for 3 h under Dean-Stark conditions with the exclusion of moisture from the air. During the reaction the mixture became turbid and after cooling to room temperature, a non-transparent, white gel was formed. The gel was filtered with suction over a glass filter and the residue, an off-white crusty compound, was crushed with a spatula, suspended in a 50:50 mixture of dry dichloromethane (containing 10% triethylamine in order to keep the solution/suspension basic) and dry ether and subjected to ultrasound in order to get a very finely divided suspension. This suspension was centrifuged and the white sediment was collected. This procedure was repeated two more times, after which white, solid **4.1** was obtained (4.72g, 13.9 mmol, 73%). ^{1}H-NMR (300 MHz, DMSO-*d6*): δ = 0.84 (t, J = 7.0 Hz, 6H), 1.30 (m, 8H), 2.98 (dt, J = 5.9 Hz, J = 8.5 Hz, 4H), 6.08 (t, J = 8.5 Hz, 1H), 6.15 (t, J = 8.3 Hz, 2H), 6.58 (d, J = 8.3 Hz, 2H), 7.21 - 7.35 (m, 5H). ^{13}C-NMR (75.48 MHz, DMSO-*d6*): δ = 13.7, 19.5, 32.1, 38.8, 59.2, 126.1, 127.1, 128.4, 143.0, 157.1. Elemental

analysis: Calc. for $C_{17}H_{28}N_4O_2$: C, 63.69; H, 8.81; N, 17.51. Found C, 63.53; H, 8.86; N, 17.34. mp.: >170 ^oC (dec.) IR (nujol mull) ν_{max} (cm^{-1}): 3343 (s, N-H), 1632 (s, amide-I), 1562 (s, amide-II).

Synthesis of 1-benzyl-3-[(3-benzylureido)phenylmethyl]urea (4.2).

This compound was prepared as described for **4.1**, starting from benzylurea and benzaldehyde. Yield 82%. White solid. ^{1}H-NMR (300 MHz, DMSO-*d6*): δ = 4.22 (d, J = 5.9 Hz, 4H), 6.25 (t, J = 8.2 Hz, 1H), 6.60 (t, J = 9.6 Hz, 2H), 6.80 (d, J = 8.1 Hz, 2H), 7.19 - 7.35 (m, 15H). ^{13}C-NMR (75.48 MHz, DMSO-*d6*): δ = 42.8, 59.4, 125.9, 126.6, 127.0, 128.1, 128.2, 140.6, 142.7, 157.0, 182.9. Elemental analysis: Calc. for $C_{23}H_{24}N_4O_2$: C, 71.13; H, 6.22; N, 14.41. Found C, 71.06; H, 6.16; N, 14.44. mp.: >170 ^oC (dec.) IR (nujol mull) ν_{max} (cm^{-1}): 3337 (s, N-H), 1630 (s, amide-I), 1559 (s, amide-II).

Synthesis of 1-butyl-3-[(3-butylureido)-*p*-chlorophenylmethyl]urea (4.3).

This compound was prepared as described for **4.1**, starting from butylurea and *p*-chlorobenzaldehyde. Yield 78%. White solid. ^{1}H-NMR (DMSO-*d6*, 300 MHz): δ = 0.85 (t, J = 7.1 Hz, 6H), 1.19 - 1.36 (m, 8H), 2.97 (dt, J = 5.9 Hz, J = 8.8 Hz, 4H), 6.10 (br s, 3H), 6.64 (d, J = 8.1 Hz), 7.30 (d, J = 8.4 Hz, 2H), 7.37 (d, J = 8.4 Hz, 2H). ^{13}C-NMR (DMSO-*d6*, 75.48 MHz): δ = 13.7, 19.5, 32.0, 38.8, 58.7, 127.9, 127.9, 131.4, 142.0, 157.0. Elemental analysis: Calc. for $C_{17}H_{27}ClN_4O_2$: C, 57.50; H, 7.70; N, 15.80. Found C, 57.53; H, 7.71; N, 15.68. mp.: >170 ^oC (dec.) IR (nujol mull) ν_{max} (cm^{-1}): 3331 (s, N-H), 1638 (s, amide-I), 1562 (s, amide-II).

Synthesis of 1-butyl-3-[(3-butylureido)-*p*-methoxyphenylmethyl]urea (4.4).

This compound was prepared as described for **4.1**, starting from butylurea and *p*-methoxybenzaldehyde. Yield 65%. White solid. ^{1}H-NMR (DMSO-*d6*, 300 MHz): δ = 0.85 (t, J = 7.1 Hz, 6H), 1.22 - 1.36 (m, 8H), 2.97 (dt, J = 6.2 Hz, J = 9.3 Hz, 4H), 3.72 (s, 6H), 6.04 - 6.11 (m, 3H), 6.50 (d, J = 8.4 Hz, 2H), 6.87 (d, J = 8.8 Hz, 2H), 7.21 (d, J = 8.8 Hz, 2H). ^{13}C-NMR (DMSO-*d6*, 75.48 MHz): δ = 13.7, 19.5, 32.1, 38.8, 55.1, 58.8, 113.4, 127.1, 134.8, 157.0, 158.3. Elemental analysis: Calc. for $C_{18}H_{30}N_4O_2$: C, 61.70; H, 8.61; N, 16.03. Found C, 61.74; H, 8.51; N, 15.90. mp.: >170 ^oC (dec.) IR (nujol mull) ν_{max} (cm^{-1}): 3345 (s, N-H), 1638 (s, amide-I), 1568 (s, amide-II).

Synthesis of 1-butyl-3-[(3-butyl-ureido)-*p*-dimethylaminophenylmethyl]urea (4.5).

This compound was prepared as described for **4.1**, starting from butylurea and *p*-dimethylamino-benzaldehyde. Yield 48%. White solid. Purification of this compound was very difficult (see elemental analysis) because of its instability. It decomposes rapidly into its starting materials, as was noted by the always present smell of the parent aldehyde. NMR reveals that, after purification, the compound is at least of 90% purity. ^{1}H-NMR (DMSO-*d6*, 300 MHz): δ = 0.87 (t, J = 7.1 Hz, 6H), 1.27 - 1.41 (m, 8H), 2.85 (s, 6H), 2.97 (d, J = 5.5 Hz, 4H), 6.05 (br s, 3 H), 6.40 (d, J = 8.1 Hz, 2H), 6.67 (d, J = 8.1 Hz, 2H), 7.11 (d, J = 8.1 Hz, 2H). ^{13}C-NMR (DMSO-*d6*, 75.48 MHz): δ = 13.7, 19.5, 32.1, 38.8, 40.3, 58.9, 112.1, 1216.5, 130.3, 149.7, 157.0. Elemental analysis: Calc. for $C_{19}H_{33}N_5O_2$: C, 62.80; H, 9.20; N, 19.30. Found C, 59.88; H, 8.78; N, 18.57. mp.: >170 ^{o}C (dec.) IR (nujol mull) ν_{max} (cm^{-1}): 3337 (s, N-H), 1630 (s, amide-I), 1559 (s, amide-II).

Synthesis of 1-butyl-3-[(3-butyl-ureido)-(p-nitrophenyl)-methyl]-urea (4.6).

This compound was prepared as described for **4.1**, starting from butylurea and *p*-nitro-benzaldehyde. Yield 79%. White solid. ^{1}H-NMR (DMSO-*d6*, 300 MHz): δ = 0.85 (t, J=7.1 Hz, 6H), 1.22 - 1.36 (m, 8H), 2.98 (dt, J = 6.2 Hz, J = 9.3 Hz, 4H), 6.15 - 6.22 (m, 3H), 6.82 (d, J = 8.1 Hz, 2H), 7.54 (d, J = 8.4 Hz, 2H), 8.20 (d, J = 8.4 Hz, 2H). ^{13}C-NMR (DMSO-*d6*, 75.48 MHz): δ = 13.7, 19.5, 32.0, 38.8, 58.9, 123.2, 127.2, 146.4, 150.9, 157.0. Elemental analysis: Calc. for $C_{17}H_{27}N_5O_4$: C, 55.92; H, 7.39; N, 19.42. Found C, 55.89; H, 7.24; N, 19.16. mp.: >170 ^{o}C (dec.) IR (nujol mull ν_{max} (cm^{-1}): 3352 (s, N-H), 1640 (s, amide-I), 1580 (s, amide-II).

References

1. The research presented in this chapter has been published: Schoonbeek, F.S.; Van Esch, J.H.; Hulst, R.; Kellogg, R.M.; Feringa, B.L. *Chem. Eur. J.* **2000**, *6*, 2633-2643.
2. Terech, P.; Weiss, R.G. *Chem. Rev.* **1997**, *97*, 3133-3159.
3. Van Esch, J.H.; Schoonbeek, F.S.; De Loos, M.; Veen, E.M.; Kellogg, R.M.; Feringa, B.L. "*Supramolecular Science: where it is and where it is going"*, NATO ASI Series, Series C: Mathematical and Physical Sciences – Vol. 527. Kluwer Academic Publishers, **1998**, 233-259.
4. (a) Clavier, G.M.; Brugger, J.-F.; Bouas-Laurent, H.; Pozzo, J.-L. *J. Chem. Soc.* **1998**, 2527; (b) Hanabusa, K.; Maesaka, Y.; Kimura, M.; Shirai, H. *Tetrahedron Lett*. **1999**,

40, 2385-2388; (c) Oda, R.; Huc, I.; Candau, S.J. *Angew. Chem. Int. Ed. Engl.* **1998,** *19*, 2689-2691; (d) Yoza, K.; Ono, Y.; Yoshihara, K.; Akao, T.; Shinmori, H.; Takeuchi, M.; Shinkai, S.; Reinhoudt, D.N. *Chem. Commun.* **1998**, 907-908.

5. (a) Hanabusa, K.; Shimura, K.; Hirose, K.; Kimura, M.; Shirai, H. *Chem. Lett.* **1996**, 885-886. (b) Hanabusa, K.; Yamada, M.; Kimura, M.; Shirai, H. *Angew. Chem. Int. Ed. Engl.* **1996**, *35*, 1949-1951.
6. (a) Van Esch, J.; Kellogg, R.M.; Feringa, B.L. *Tetrahedron Lett.* **1997**, *38*, 281; (b) Van Esch, J.; De Feyter, S.; Kellogg, R.M.; De Schryver, F.; Feringa, B.L. *Chem. Eur. J.* **1997**, *3*, 1238-1243.
7. (a) De Loos, M.; Van Esch, J.; Stokroos, I.; Kellogg, R.M.; Feringa, B.L. *J. Am. Chem. Soc.* **1997**, *119*, 12675-12676; (b) Van Esch, J.H. Schoonbeek, F.S.; De Loos, M.; Kooijman, H.; Kellogg, R.M.; Feringa, B.L. *Chem. Eur. J.* **1999**, *5*, 937-950.
8. Snijder, C.M.; De Jong, J.C.; Meetsma, A.; Van Bolhuis, F.; B.L. Feringa, *Chem. Eur. J.* **1995**, *1*, 594-597.
9. Menger, F.M.; Yamasaki, Y.; Catlin, K.K.; Nishimi, T. *Angew. Chem. Int. Ed. Engl.* **1995**, *34*, 585-586.
10. Zehavi, U.; Ben-Ishai, D. *J. Org. Chem.* **1961**, *26*, 1097-1101.
11. (a) Jadzyn, J.; Stockhausen, M.; Zywucki, B. *J. Phys. Chem.*, **1987**, *91*, 754-757; (b) Doig, A.J.; Williams, D.H. *J. Am. Chem. Soc.* **1992**, *114*, 338-343.
12. Takahashi, A.; Sakai, M.; Kato, T. *Polym. J.* **1980**, *12*, 335-341.
13. Garner, C.M.; Terech, P.; Allegraud, J.-J.; Mistrot, B.; Nuygen, P.; De Geyer, A.; Rivera, D. *J. Chem. Soc. Far. Trans.* **1998**, *94*, 2173-2179.
14. Murata, K.; Aoki, M.; Suzuki, T.; Harada, T.; Kawabata, H.; Komori, T.; Ohseto, F.; Ueda, K.; Shinkai, S. *J. Am. Chem. Soc.* **1994**, *116*, 6664-6676.
15. Evaluation of the temperature dependence of the critical aggregation concentrations or the solubility by means of a phase separation model or Schraders equation is only justified when the exact solute concentration at the melting temperature is known. Apparently, in this case the melting process is not completed and hence the solute concentration at the melting point as determined by the dropping ball method is not equal to the given concentration.
16. (a) Hartman, P.; Bennema, P. *J. Cryst. Growth* **1980**, *49*, 145-156; (b) Weissbuch, I.; Popovitz-Biro, R.; Lahav, M.; Leiserowitz, L. *Acta Crystallogr.* **1995**, *B51*, 115-148.
17. Dobrowolsky, J.Cz.; Jamróz, M.H.; Mazurek, A.P. *Vibr. Spectrosc.* **1994**, *8*, 53.
18. The amide-I absorption for **4.1** at low concentration in chloroform shows a quite large deviation (23 cm^{-1}) from the value for **4.1** at low concentration in dichloroethane. This is most likely due to the fact that chloroform acts as a (weak) hydrogen bond donor. (a) Mido, Y. *Spectrochim. Acta* **1973**, *29A*, 431-438; (b) Harnagea, E.I.; Jagodzinski, P.W. *Vibr. Spectrosc.* **1996**, 169.
19. Quanta97/CHARMm is a product of Molecular Simulations Inc., San Diego, USA. Internet: http://www.msi.com
20. (a) Scaringe, R.P.; Perez, S. *J. Phys. Chem.* **1987**, *91*, 2394-2403; (b) Perlstein, J. *J.*

Am. Chem. Soc. **1994**, *116*, 11420-11432; (c) Lauher, J.W.; Chang, Y.-L.; Fowler, F.W. *Mol. Cryst. Liq. Cryst*. **1992**, *211*, 99-109.

21. (a) Chang, Y.-L.; West, M.-A.; Fowler, F.W.; Lauher, J.W. *J. Am. Chem. Soc.* **1993**, *115*, 5991-6000; (b) Kolodziejski, W.; Wawer, I.; Wozniak, K.; Klinowski, J. *J. Phys. Chem.* **1993**, *97*, 12147-12152; (c) Carr, A.J.; Melendez, S.J.; Geib, S.J.; Hamilton, A.D. *Tetrahedron Lett.* **1997**, *39*, 7447-7450; (d) Schauer, C.L.; Matwey, E.; Fowler, F.W.; Lauher, J.W. *J. Am. Chem. Soc.* **1997**, *119*, 10245-10246; (e) Zhao, X.; Chang, Y.-L.; Fowler, F.W.; Lauher, J. W. *J. Am. Chem. Soc*. **1990**, *112*, 6627-6634.
22. An examination of 27 crystal structures of non-cyclic urea compounds deposited in the Cambridge Crystallographic Database revealed that the carbonyl groups of adjacent urea fragments participating in hydrogen bonding are most likely to be colinear (angle α, Figure 4.8). In addition to that, the dihedral N-C-O···H angle (angle β, Figure 4.8) is either (close to) 0^o (24 cases) or (close to) 90^o (3 cases).
23. The same is observed for *N,N'*-dimethylurea, only at much higher concentrations (0.2 – 1.0 M). Haushalter, K.A.; Lau, J.; Roberts J.D. *J. Am. Chem. Soc.* **1996**, *118*, 8891-8896.
24. Deans, R.; Cooke, G.; Rotello V.M. *J. Org. Chem.* **1997**, *62*, 836-839.
25. The fact that a NOE enhancement can be either positive or negative (or even zero) has to do with the correlation time of tumbling of the molecule or, in this case, the aggregate and hence is related to the size. Any advanced textbook on NOE NMR spectroscopy will provide a thorough explanation. See for example D. Neuhaus and M. P. Williamson *The Nuclear Overhauser Effect*, VCH publishers, Weinheim, **1989**, 31 - 39.
26. (a) M.D. Sefcik, J. Schaefer, E.O. Stejskal, R.A. McKay *Macromolecules* **1980**, *13*, 1132-1137; (b) H. Schönherr, P.J.A. Kenis, J.F.J. Engbersen, S. Harkema, R. Hulst, D.N. Reinhoudt, G.J. Vancso *Langmuir* **1998**, *14*, 2801-2809.
27. It is expected that the spectral characteristics of translation (P1) aggregates are different from those of $P2_1$ and Pa aggregates. However, highly resolved spectra are only obtained in solution, under the conditions of fast exchange. In the solid state no exchange takes place, but the resolution is in these cases drastically reduced.